A Stellar Model

For a $2.75 M_\odot$ Homogeneous Main-Sequence Star

Xin Xiang

PHYSICS 3021 PAPER PROJECT (FALL 2021)

Xin Xiang, Georgia Institute of Technology

November 22, 2021

Table of Contents

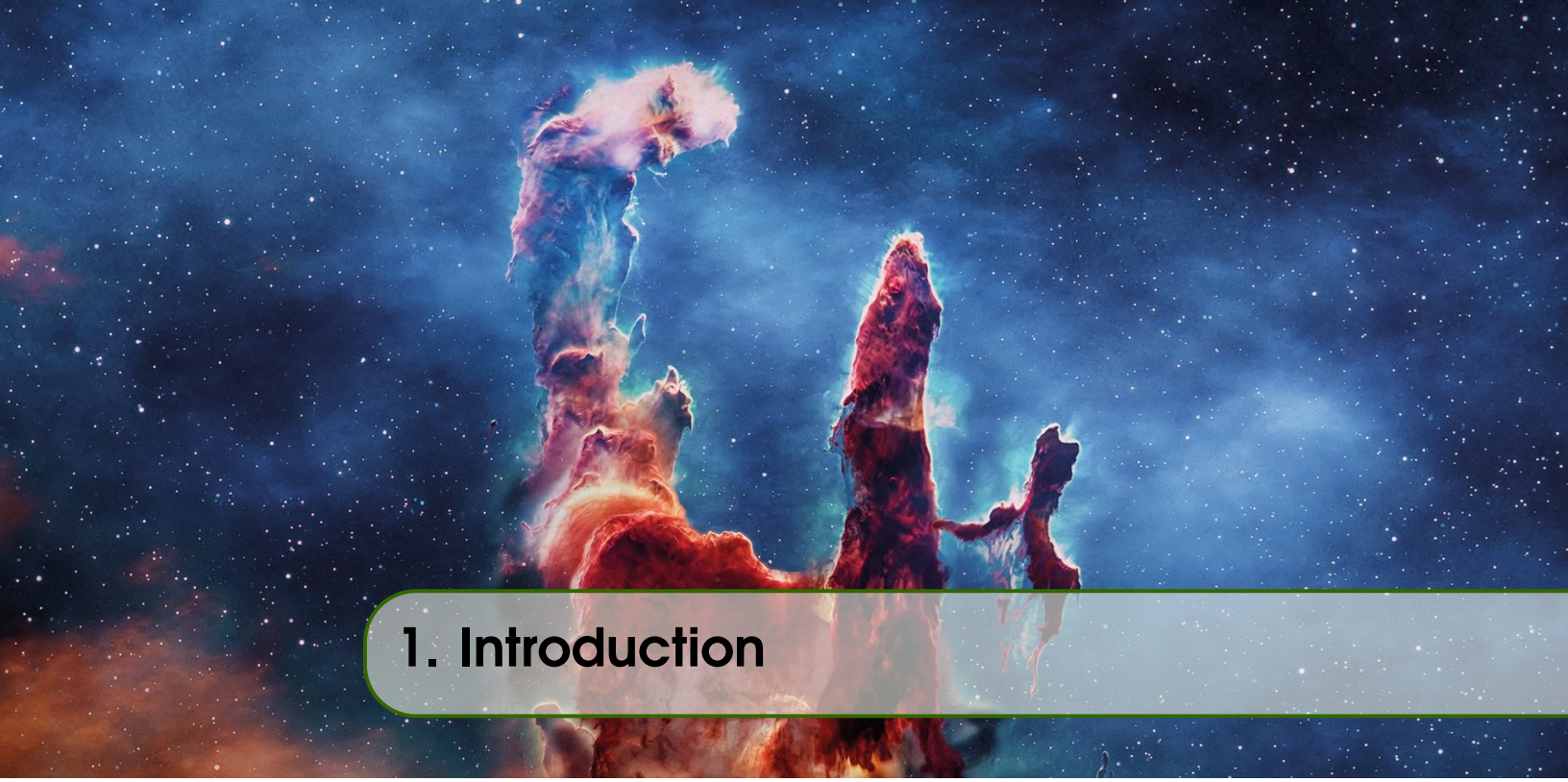

1. Introduction

A star is a spherical astronomical object consisting of luminous plasma held by its own gravity [6]. The Sun is the nearest star to the Earth. Many bright stars can be seen on the night sky as fixed points of light as they are significantly far away from the Earth. The nearest star from the Sun is Proxima Centauri, which is located 4.25 light-years (1.30 pc) away in the southern constellation of Centaurus[5]. Stars are formed in Molecular Cloud through various mechanical processes, including gravitational collapse and contraction of interstellar matter. They reach hydrostatic equilibrium after these mechanical processes as Proto-Star stage and then evolve into the main sequence after igniting the hydrogen fusion in the core. A star the size of our Sun takes as long as 50 million years to evolve from the beginning of the collapse to Main Sequence. Our Sun will stay on the main sequence for approximately 10 billion years fusing hydrogen to helium in the core providing the energy outflow and pressure that keep it from collapsing under its own weight.

Main Sequence stars span a wide range of luminosities and surface temperatures and can be classified according to those characteristics. The smallest main sequence stars, known as red dwarfs, contain as little as 10% the mass of the Sun and emit only 0.01% as much energy, glowing faintly at temperatures around 3000K. Red dwarfs have a life span of tens of billions of years and are by far the most numerous stars in the Universe. On the other hand, hypergiants, the most massive main-sequence stars, have a life span of only a few million years and are extremely rare in today's Universe. The entire Milky Way galaxy contains only a handful of hypergiants [8]. They are hundreds of times more massive than the Sun, have surface temperatures of more than 30,000 K, and emit hundreds of thousands of times more energy than the Sun. In general, all evolutionary stages are relatively faster in stars of high mass, and slower in those of low mass [12]. In order to understand how stars evolve in the Main Sequence, we need to know the interior environment of stars. However, we are not able to directly probe the interiors of stars. Thus, modeling the interior parameters (such as mass, luminosity, temperature, and density) whose exterior values match the observational constraints is a crucial method to describe the internal structure in detail and make predictions about the future evolution of the star.

In this paper, we describe a homogeneous quasi-static stellar structure model for a $2.75M_{\odot}$ Main Sequence Star (labeled $Star^{*}$) using the four basic first-order differential equations: two represent how matter and pressure vary with radius; two represent how temperature and luminosity vary with radius. The detailed description of the model for the interior structure given the star's surface condition, as well as the estimation for the fusion reaction status in the core, are presented in Chapter 2. The comparisons of the model to a real star with the same mass are discussed in Chapter 2.3.

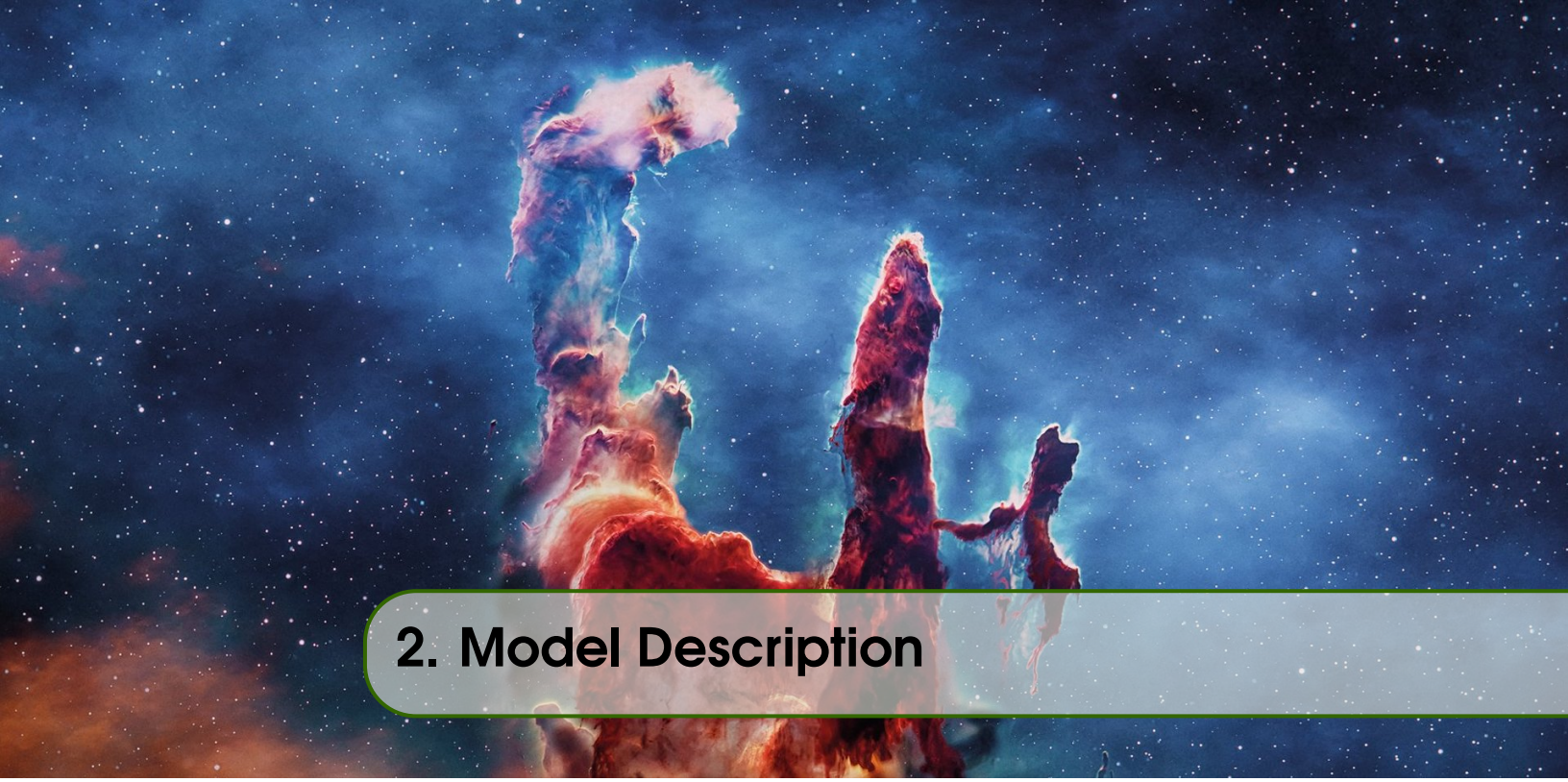

2. Model Description

2.1 Surface

In this section, we will discuss the surface appearance and the spectral type of $Star^*$. The surface conditions for the $star^*$ comparing to that of a $1.00M_\odot$ star (labeled $star1$) are shown in the table 2.1. where $M_\odot = 1.99 \cdot 10^{33}(g)$ is the mass of the Sun.

2.1.1 Luminosity, Effective Temperature, and Magnitude

A star in thermal equilibrium is approximately a blackbody that absorbs all electromagnetic radiation and emits radiation whose spectrum depends on its temperature. The effective temperature T_{eff} of a star is defined as the temperature needed for a blackbody with the same radius R as the star to have the same luminosity L[10]. The Planck distribution function that describes the spectrum of radiation

Table 2.1: The surface Condition of the model for $star^*$ and $star1$. M_{tot}, R_{tot}, L_{tot}, and T_{eff} are the mass, radius, luminosity, and effective temperature of the stars. X is the mass ratio of Hydrogen atoms. Y is the mass ratio of Helium atoms. Z is the mass ratio of the Metals. $M_\odot = 1.99 \cdot 10^{33}(g)$, $R_\odot = 6.96 \cdot 10^{10}(cm)$, and $L_\odot = 3.846 \cdot 10^{33}(ergs/s)$ are parameters for the Sun.

Parameters	$star^*$	$star^1$
M_* (g)	$2.75M_\odot$	$1.00M_\odot$
R_* (cm)	$1.51R_\odot$	$1.02R_\odot$
L_* (ergs/s)	$83.14L_\odot$	$0.86L_\odot$
T_{eff} (K)	14170.8	5500.2
X	0.700	0.700
Y	0.292	0.292
Z	0.008	0.008

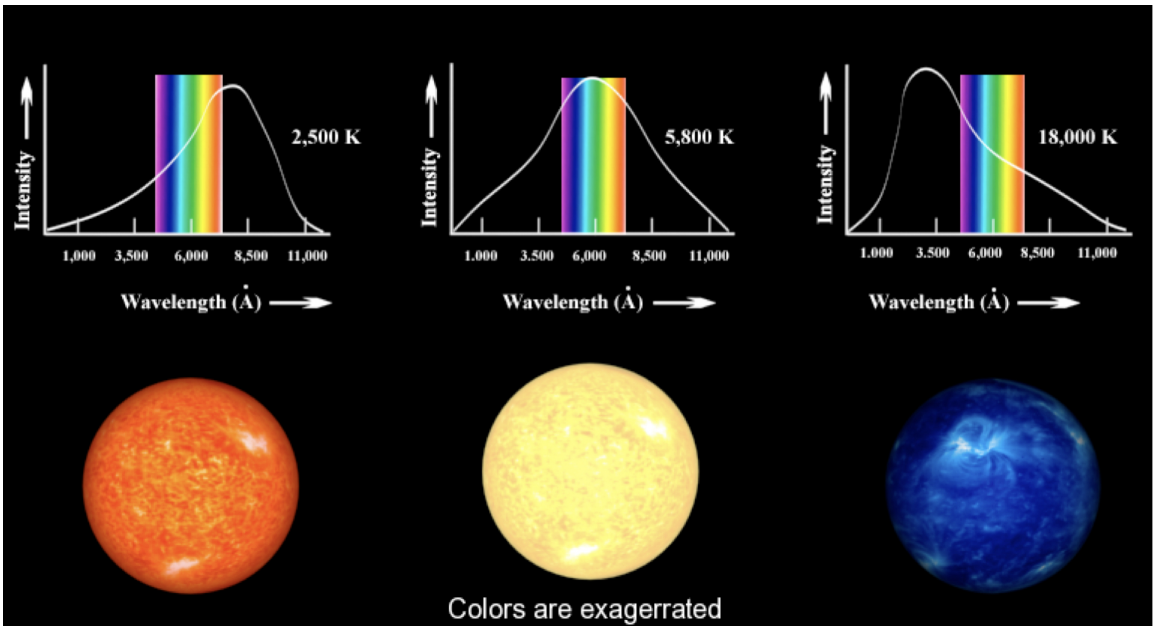

Figure 2.1: The blackbody radiation. Credit: [11]

for a blackbody is given by:

$$B(\lambda, T) = \frac{2hc^2}{\lambda^5 e^{\frac{hc}{\lambda kT}} - 1} \tag{2.1}$$

, where k is the Boltzmann constant, h is the Planck constant, and c is the speed of light in the medium. Figure 2.1 shows the plots of spectral radiation in terms of wavelength for three different temperature values. Two laws can be derived from the Planck distribution function. One is Wien's law that describes the maximum wavelength emitted by a blackbody, at which the function 2.1 is at its maximum:

$$\lambda_{max} = \frac{0.29Kcm}{T} \tag{2.2}$$

It explains that the hotter stars are blue and coolers ones are red. Using Wien's law, we can estimate that the maximum wavelength emits by $Star^*$ and $Star1$ are $205nm$ (Ultraviolet) and $527nm$ (Green-yellow Light). $Star^*$ appears blueish while $Star1$ appears yellowish. The other law that can be derived is Stefan-Boltzmann Law, which gives the flux F (the total power output per unit area $ergs/s/cm^2$) by integrating the Planck distribution 2.1 with all wavelength:

$$F = \sigma T^4 \qquad (\sigma = 5.67 \times 10^{-5} ergs^{-1} cm^{-2} K^{-4}) \tag{2.3}$$

Thus the luminosity (the total power output per second $ergs/s$) can be written as:

$$L = 4\pi R^2 \sigma T^4 \tag{2.4}$$

From the table, we see that $Star^*$ is 2.58 times hotter and 1.48 times larger than $Star1$, indicating that the $Star^*$ should be $2.58^4 * 1.48^2 = 96.56$ times more luminous than $Star1$, in agreement with

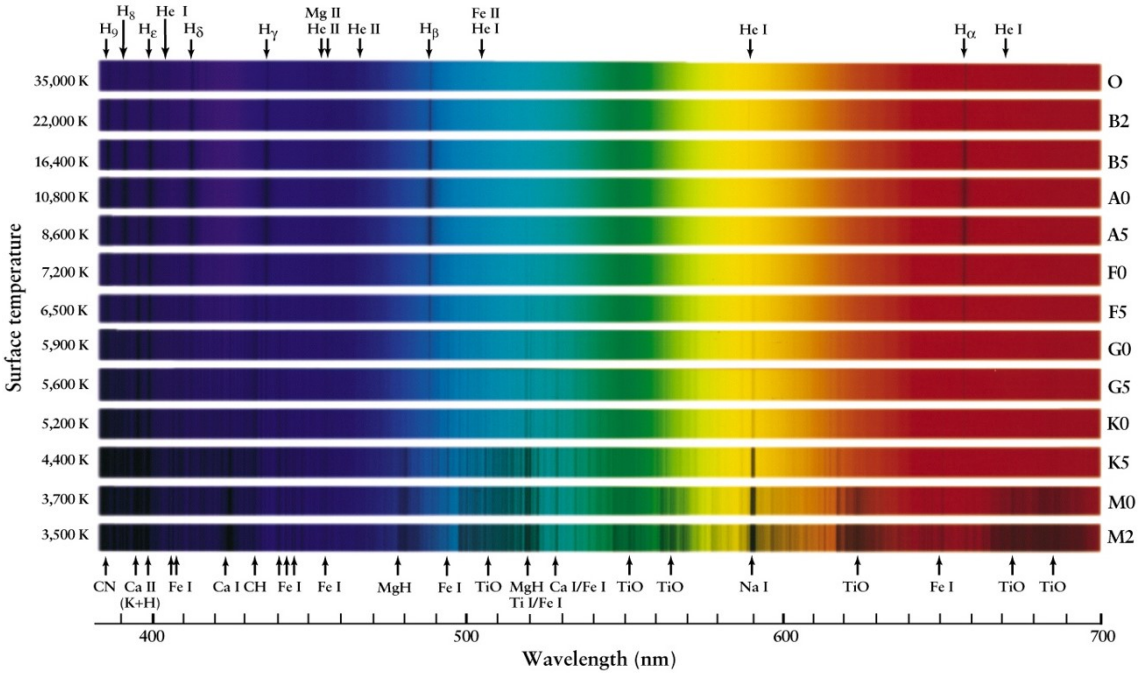

Figure 2.2: The optical spectral characteristics change with T_{eff}. Credit: [9]

the data given in the table. It can also be inferred from the equation 2.4 that a star with a higher temperature emits more energy at all wavelengths than a cooler one. If we put them in the night sky at the same distance from us, $Star^*$ will be much brighter than $Star1$. In astronomy, we use magnitude to measure the brightness of an object[4]. Apparent magnitude (m) depends on an object's intrinsic luminosity and its distance from the Earth, while absolute magnitude (M^m) describes its intrinsic luminosity and is equal to apparent magnitude if the object were placed on 10 parsecs from the Earth. The relationship of the magnitude of two stars is given by the formula:

$$m_1 - m_2 = 2.5log(\frac{F_2}{F_1}) \tag{2.5}$$

F_1 and F_2 are the total power output observed on the Earth F_{obs} at a distance d from the stars:

$$F_{obs} = \frac{L}{4\pi d^2} \tag{2.6}$$

The equation (2.5) is the modern definition of magnitudes whose difference is 5, corresponding to a flux ratio of 100. The lower the magnitude, the higher the flux. By substituting equation (2.6) in equation (2.5) and setting the distance of the second object to be 10 parsecs with the same luminosity, we can show that the difference between the apparent magnitude and the absolute magnitude of a star is:

$$m - M = 5log(\frac{d}{10}) \tag{2.7}$$

From equation (2.5) and equation (2.6), it can be easily derived that difference of the absolute magnitude of two stars is:

$$M_1 - M_2 = 2.5log(\frac{L_2}{L_1}) \tag{2.8}$$

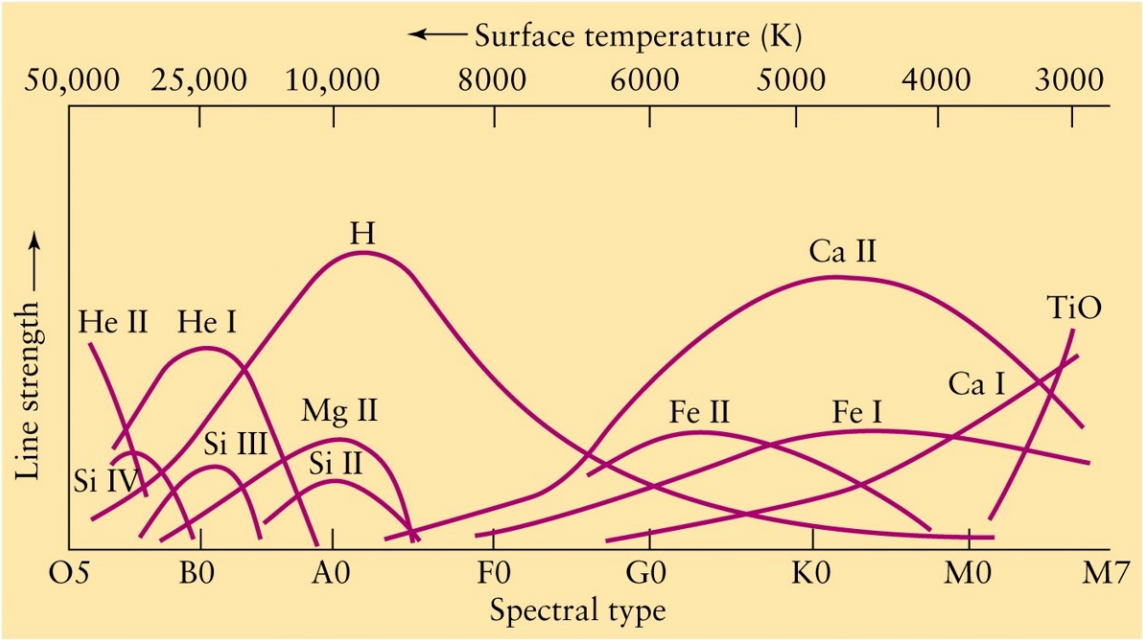

Figure 2.3: The approximate line intensity as a function of T_{eff}. Credit: [9]

Knowing that the absolute magnitude of $Star1$ is 4.75^m, using this equation, we can derive that the absolute magnitude of $Star^*$ is -0.21^m.

2.1.2 Spectral Classification

The primary cause of differences in stellar spectra is the effective temperatures that influence two processes: excitation and unionization of atoms described by Boltzmann equation and Saha Equation. Boltzmann equation gives the ratio of the number density of two energy-levels of a given ion in gas at temperature T:

$$\frac{N_b}{N_a} = \frac{g_b}{g_a} e^{-(E_b - E_a)/(kT)} \tag{2.9}$$

, where $g_n = 2n^2$is the number multiplicity of the level, E is the energy of the level. From this equation, we see that the population of the higher energy level atoms is larger for a hotter star. Take hydrogen lines as an example. The transition lines from the n = 1 level to a higher level are found in the Ultraviolet part of the spectrum, called the Lyman lines ($L_\alpha, L_\beta, L_\gamma, etc.$). From the n = 2 level to higher are called the Balmer series ($H_\alpha, H_\beta, H_\gamma$, etc.) in the Visible part of the spectrum. For a cool star, almost all of the hydrogen atoms are in their ground state, and the Balmer lines are very weak, as well as Lyman lines, since not many photons have energy high enough for the atoms to emit Ultraviolet. For hotter stars ($T_{eff} \sim 10000K$), the population of hydrogen atoms in the n = 2 level is very large, and their Blamer lines are intense. Figure 2.2 demonstrate this trend for hydrogen lines.

Saha equation gives the ratio of the atoms' number density of two adjacent ionization states:

$$\frac{N_{i+1}}{N_i} = \frac{2kTZ_{i+1}}{P_e Z_i} * \left(\frac{2\pi m_e kT}{h^2}\right)^{\frac{3}{2}} e^{-\chi_i/kT} \tag{2.10}$$

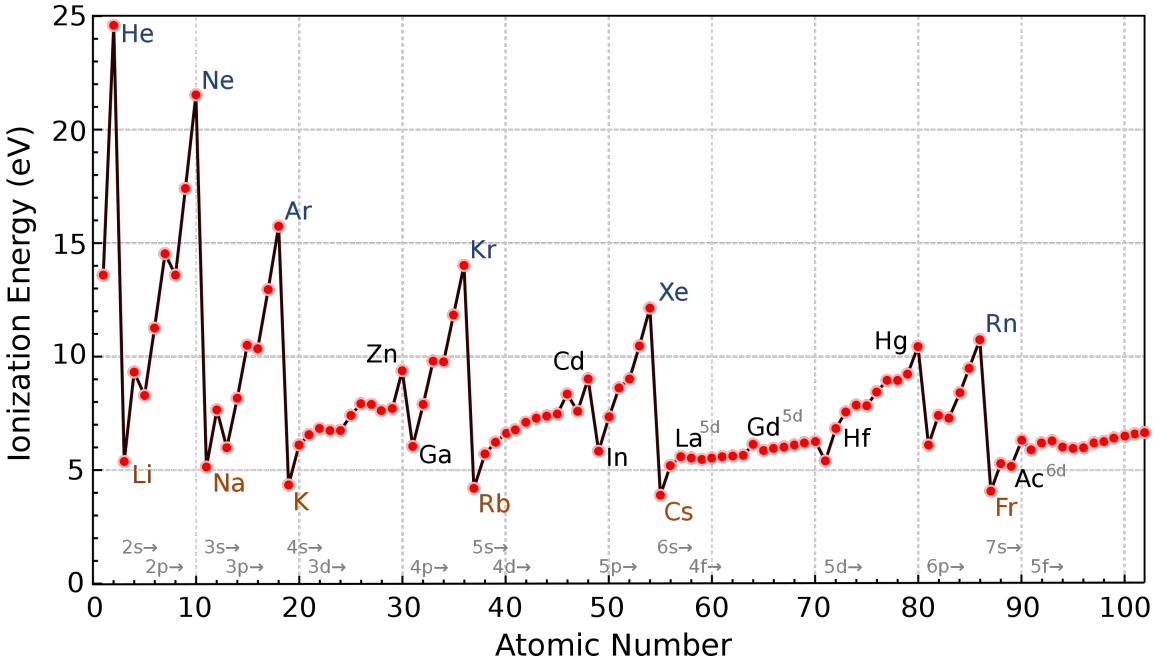

Figure 2.4: Ionization energy for different elements Credit: [2]

, where n_e, Z, and χ are number of electrons, partition functions, and ionization potential (χ = 13.6 for hydrogen atoms). The Boltzmann and Saha equations describe two contributors that explain the trend of spectral lines for all the different elements in figure 2.3. The portion of neutral hydrogen found in energy level n = 2 maximized at a temperature around 10000K. For lower temperatures, the population of n = 2 level among neutral hydrogen atoms is smaller. While for higher temperatures, the population of neutral hydrogen atoms decreases. Thus the combination of the two processes (excitation and ionization) contributes to the concave down curves of the line strength for all the different elements. The position of the curve's maximum, however, depends on the ionization energy of different elements shown in figure 2.4. The larger the ionization energy of an atom, the hotter the curve's maximum will be. This explains that, for example, FeII lines are strong in cooler stars while HeII lines are strong in hotter stars.

The stars are classified into different spectral types: O, B, A, F, G, K, M going from hotter to cooler effective temperature. Figure 2.3 shows the intensity of spectral lines for different elements as a function of temperature. From this figure, we can tell that $Star*$ is approximately a B6 star, whose Hydrogen lines are strongest in its optical spectrum. Assume that the $Star*$ has the same composition as the Sun's (X = 0.735, Y = 0.248, Z = 0.017), $Star*$ will have strong Blamer lines and He lines. The position of $Star*$ determined by its temperature in the H-R diagram is shown in the figure 2.5. For main sequence stars, the masses are lower, moving from the upper left to the lower right in the HR diagram. The graph on the right in the figure 2.5 shows the spectral type of $Star^*$ determined by its mass, which is approximately an $A2$ star. The results are quite different from that is determined by its temperature. The temperature of real main-sequence stars with mass $M = 2.75 M_\odot$ should have been lower than the given data in table 2.1 or the mass of the real main-sequence stars with temperature $T = 14170.8$ should have been larger according to [3].

The massive main sequence stars have higher surface temperatures and thus emit more power

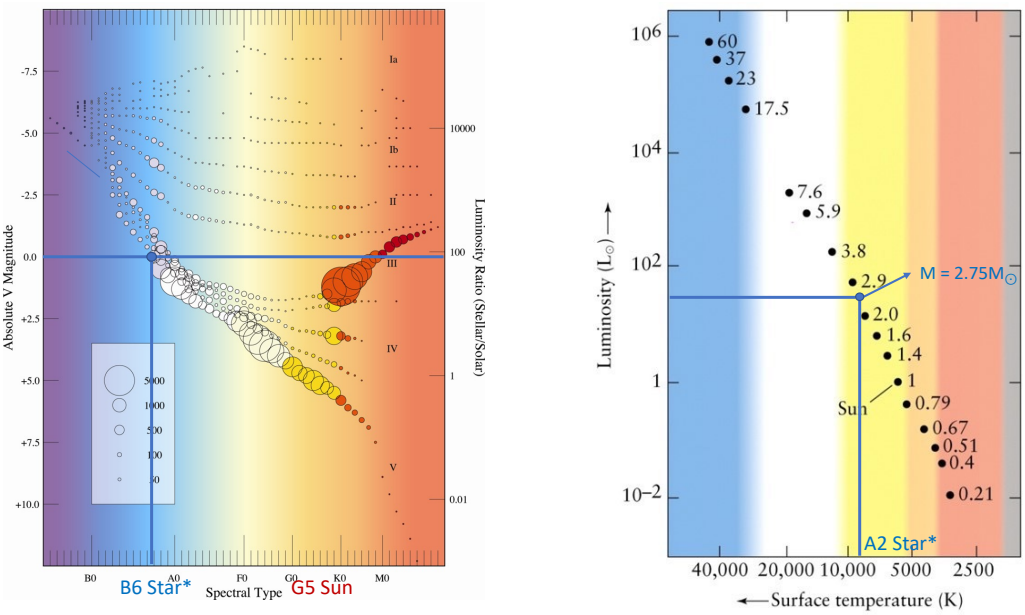

Figure 2.5: H-R diagram showing the position of *Star*∗. The graph on the left shows the spectral type determined by the temperature. The graph on the right shows the spectral type determined by the mass. Credit: [12]

than low-mass stars with lower surface temperatures. Hence, more massive stars will have a shorter lifespan in the main sequence because the energy generation from the nuclear reaction that consumed hydrogen in the core is at a higher rate. The time for stars to stay in the main sequence is approximately:

$$t_{ms} = 10^{10} \left(\frac{M}{M_\odot}\right) \left(\frac{L}{L_\odot}\right)^{-1} yr \tag{2.11}$$

This indicates that *Star** will stay on the main sequence for 1.82×10^{10} years.

2.2 Interior: Structure and Fusion

In this section, we will model the parameters (mass, pressure, temperature, and luminosity) change inside the *Star** and discuss the fusion reaction environment in the central core.

2.2.1 Modelling Parameters Change with Radius

We assume the star is spherically symmetric. By solving the four basic equations, commonly called the equation of stellar structure, the interior parameters of the stars in terms of distance from the center can be determined given the surface condition. In this section, we will discuss these four equations and present the model results for the parameters of *Star**.

Hydrostatic Equilibrium Equation

In a stable star, the pressure at every internal point must counterbalance the gravitational force of the stellar layer above that point. Assume a mass element of thickness dr and area dA at a distance $r = R/R_*$ (normalized radius) from the center of the star. The mass of the element is $\rho(r)dAdr$, the upward pressure is $P(r)$, the downward pressure is $P(r)+dP$. Thus the total force act on it is:

$$P(r)dA - (P(r)+dP)dA - \rho(r)dAdrg(r) = 0 \tag{2.12}$$

, where $g(r) = \frac{GM(r)}{r^2}$ is the gravitational acceleration. This equation can be simplified to obtain the hydrostatic equilibrium equation:

$$\frac{dP(r)}{dr} = -\frac{GM(r)\rho(r)}{r^2} \tag{2.13}$$

Mass Conservation Equation

The hydrostatic equilibrium equation depends on mass at radius r. To solve the equation, we need to know the mass distribution inside the star. Consider a shell of thickness dr at radius r. The mass of this shell is:

$$dM(r) = \rho(r)dV = \rho(r)4\pi r^2 dr \tag{2.14}$$

This can be simplified to obtain the equation of mass conservation:

$$\frac{dM(r)}{dr} = 4\pi r^2\rho(r) \tag{2.15}$$

Radiative Energy Transport Equation

We assume that all of the energy is transported by the radiation process. The rate of energy is supplied to a star as a whole, and at each point within it must equal the energy loss by radiation. This balance of heat gain and heat loss is called the Thermal Equilibrium. The radiation can be described by Planck Law in equation 2.1. The total power output per unit area is given by the Stefan-Boltzmann Law in equation 2.3. The temperature gradient can be derived using the two Law: (detail derivation can be seen in the sections 3.8 and 5.2 of the book [10])

$$\frac{dT(r)}{dr} = -\frac{3\kappa(r)\rho(r)L(r)}{64\sigma T^3\pi r^2} \tag{2.16}$$

, where $\kappa(r)$ is the Opacity function of the radius r.

Energy Conservation Equation

The source of energy for a stable star is solely thermonuclear fusion. Thus the total luminosity generated inside a spherical shell with thickness dr at radius r must equal the energy generation rate of the nuclear fusion from that shell. Assume that we are given the nuclear production rate per unit mass $\varepsilon(r)$, the energy generated in the shell is:

$$dL(r) = \varepsilon(r)dM(r) = \varepsilon(r)4\pi r^2\rho(r) \tag{2.17}$$

This can be simplified to obtain the energy conservation equation:

$$\frac{dL(r)}{dr} = 4\pi r^2\rho(r)\varepsilon(r) \tag{2.18}$$

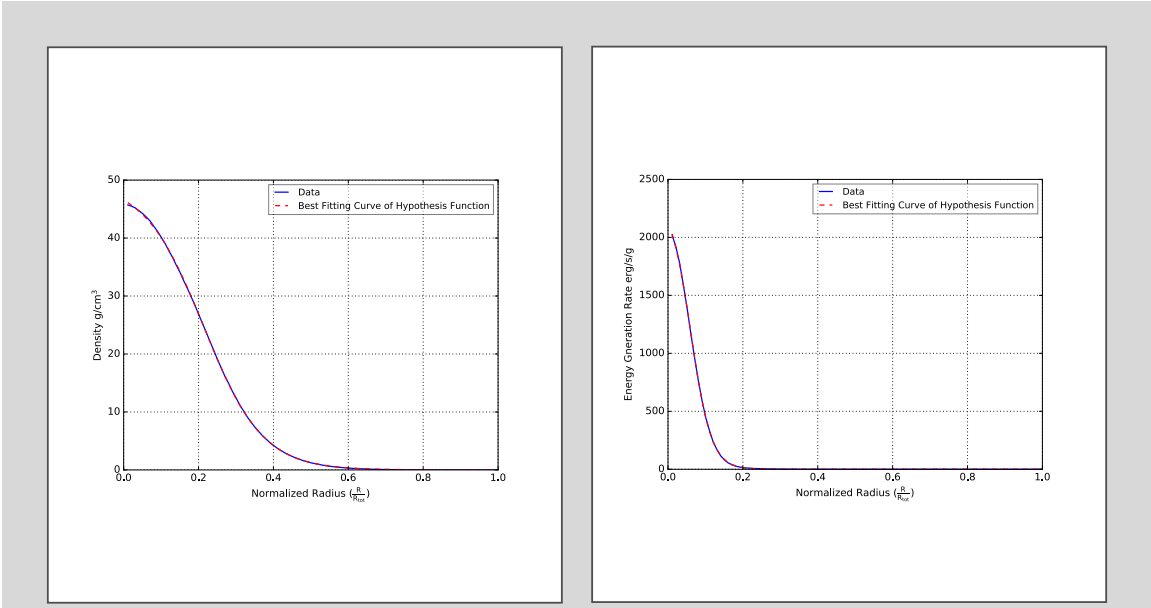

Figure 2.6: Fitting curves for Density (ρ) and Energy Generation Rate (ε)

In conclusion, the four basic equations and other ingredients needed to calculate the stellar model is summarized by:

$$\bullet\ \frac{dP(r)}{dr} = -\frac{GM(r)\rho(r)}{r^2} \qquad \bullet\ \frac{dM(r)}{dr} = 4\pi r^2\rho(r)$$

$$\bullet\ \frac{dT(r)}{dr} = -\frac{3\kappa(r)\rho(r)L(r)}{64\sigma T^3\pi r^2} \qquad \bullet\ \frac{dL(r)}{dr} = 4\pi r^2\rho(r)\varepsilon(r)$$

$$Provided\ Ingredients: \ \kappa(r);\ \varepsilon(r);\ \rho(r)$$

$$Boundary\ Conditions:$$

$$L(r\to 0) = 0 \quad L(r\to 1) = L_{tot} \qquad M(r\to 0) = 0 \quad M(r\to 1) = M_{tot}$$

$$P(r\to 1) = 0 \quad T(r\to 1) = T_{eff} \tag{2.19}$$

In this paper, we are provided the data for all the parameters inside the *Star**. In reality, we need to use the formula for $\rho(r)$, $\kappa(r)$, and $\varepsilon(r)$ to solve the four basic equations. From the data given for these three ingredients, we can make a hypothesis that the function of $\rho(r)$, $\varepsilon(r)$ and $\kappa(r)$ can be written in the form:

$$Hypothesis\ for\ \rho\ and\ \varepsilon = \frac{a}{b+ce^{dr}} \tag{2.19}$$

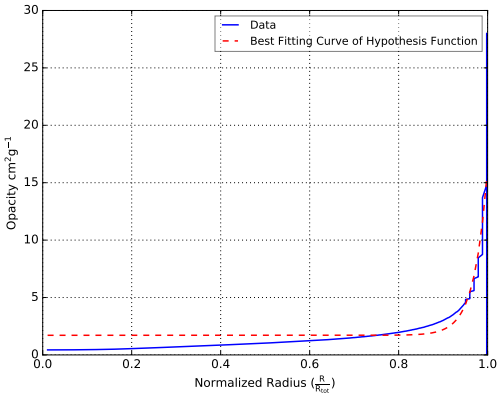

Figure 2.7: Fitting curves for Opacity (κ)

And because the Opacity should be inverse proportional to the Density:

$$Hypothesis\ for\ \kappa = xe^{yr} + z \tag{2.20}$$

, where a, b, c, d, x, y, z are constants that needed to fit with the data. By using the non-linear least squares to fit the hypothesis functions with the data, we found the equations:

$$\rho(r) = \frac{253.71}{5.11 + 0.34e^{12.71r}} \tag{2.21}$$

$$\varepsilon(r) = \frac{6351.56}{2.71 + 0.29e^{36.74r}} \tag{2.22}$$

The performance of the fitting curve is shown in figure 2.6. However, for the Opacity, we haven't found a perfect fit. The reason may due to that the hypothesis does not match the real function well. Nevertheless, the best fit for this hypothesis is:

$$\kappa(r) = 2.84 \cdot 10^{-14} e^{33.87r} + 1.71 \tag{2.23}$$

The fitting curve for Opacity function is shown in figure 2.7. In reality, we need to use these three functions as well as the boundary conditions to solve the four differential equations. As for simplicity, the data of pressure, mass, temperature, and luminosity of $Star^*$ are given. We directly plot them as a function of normalized radius in the figure 2.8. We define the Core region to be 99% of the luminosity produced. From the data, we see that the Core region is at $R_{core} = 0.27R_{tot}$, with volume ($V_{core} = 9.70 \times 10^{31} cm^3 = 1.99\% \times V_{tot}$) and mass ($M_{core} = 2.53 \times 10^{30} kg = 1.27M_{\odot} = 46.18\%M_{tot}$). The convective zone has $dlnP/dlnT \leq 2.5$. In the figure 2.8, we can see that 63% of the core is convective. The interior mass of $Star^*$ increase slower as radius getting larger, indicating that the density is dropping. The central core Temperature and Pressure are $2.45 \times 10^7 K$ and $1.50 \times 10^{17} dynes/cm^2$ and decrease rapidly out to the surface.

We assume that the composition of the $Star^*$ is homogeneous. Using the given data for the core density $\rho_{core} = 45.7 g/cm^3$, we can calculate the core Pressure by the formula:

$$P = \frac{N}{V}kT \qquad (k = 1.38 \times 10^{-16} erg/K) \tag{2.24}$$

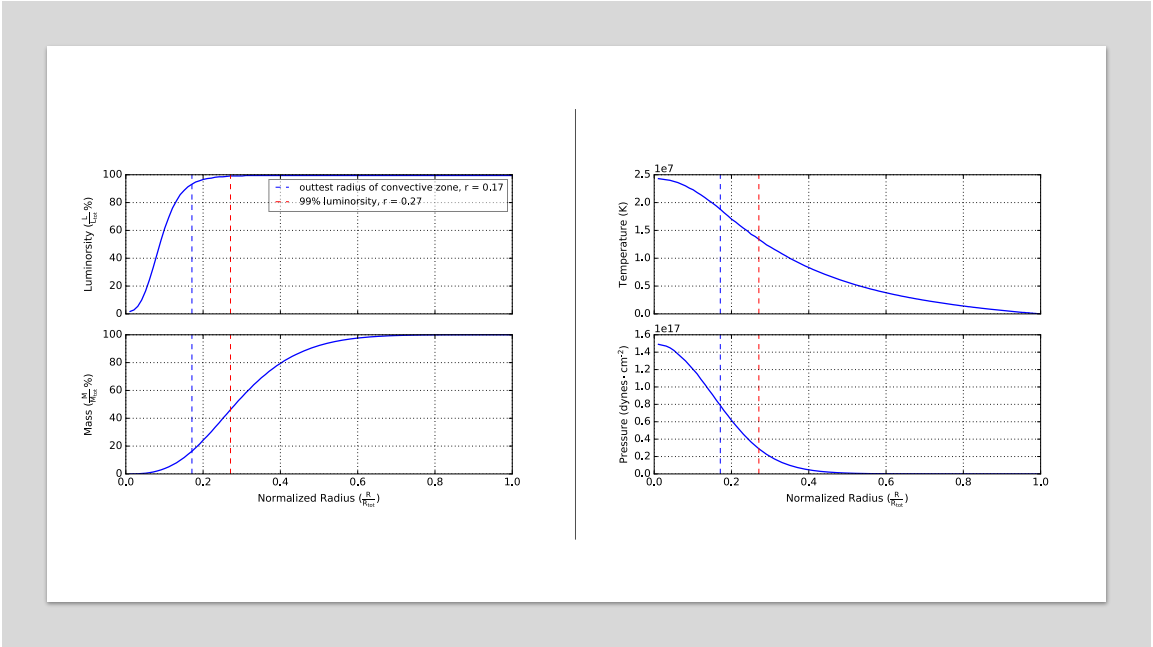

Figure 2.8: The Stellar Structure for $Star^*$

, where $\frac{N}{V}$ is the total number of particles per unit volume. Assuming the average atomic weight of the metals is 16, the total number of particles is thus:

$$N = 2X + 3/4Y + 1/2Z \tag{2.25}$$

And thus,

$$\frac{N}{V} = (2X + 3/4Y + 1/2Z)\frac{\rho}{m_H} \tag{2.26}$$

, where $m_H = 1.67 \times 10^{-27} g$ is the mass of hydrogen atoms. Using the core condition for density ρ_{core} and abundance values $X = 0.700, Y = 0.292, Z = 0.008$, we can calculate the core pressure $P_{core} = 1.5 \times 10^{17} dynes/cm^2$, which is in agreement with the data given in the model.

2.2.2 Fusion

Main sequence stars burn hydrogen to helium in their core through nuclear reactions. Two sets of reactions are involved: Proton-Proton (PP) Chains and CNO cycles. The PP Chains are the main energy generation for main-sequence stars with mass smaller than $1.5M_\odot$, while CNO cycles dominate for more massive stars [10].

The Proton-Proton Chains consists of a series of thermonuclear reactions: PP-I, PP-II, and PP-III, by which hydrogen is transformed into helium. Among all the three PP chains, PP-I has chances of 69% to happen in the core, which is when ^{3}He nucleus fuse with another ^{3}He nucleus to produce ^{4}He nucleus. PP-II and PP-III chains have chances of 31% to happen when ^{3}He nucleus reacts with

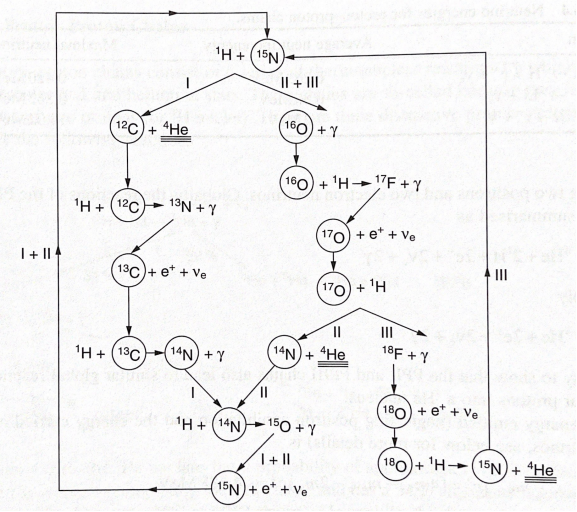

Figure 2.9: CNO cycles. Credit: [10]

a ^{4}He nucleus to produce ^{7}Be nucleus. ^{7}Be nucleus will then react with a free electron 99.7% of the time leading to PP-II chain, or react with a proton 0.3% of the time leading to PP-III. The PP chains reaction are summarized by:

$$
\begin{aligned}
&^1H + ^1H \rightarrow ^2H + e^+ + \nu \\
&^2H + ^1H \rightarrow ^3He + \gamma \\
&PP-I\,(69\%): && ^3He + ^3He \rightarrow ^4He + 2^1H \\
&(31\%): && ^3He + ^4He \rightarrow ^7Be + \gamma \\
&PP-II(31\% \times 99.7\%): && ^7Be + e^- \rightarrow ^7Li + \nu_e \\
& && ^7Li + ^1H \rightarrow 2^4He \\
&PP-III(31\% \times 0.3\%): && ^7Be + ^1H \rightarrow ^8B + \gamma \\
& && ^8B \rightarrow 2^4He + e^+ + \nu_e
\end{aligned}
\tag{2.27}
$$

The energy generation rate of PP-Chain $\varepsilon_{pp}(ergs/g/s)$is given by:[12].

$$
\varepsilon_{pp} = C_{pp}\rho X^2 \left(\frac{10^6}{T}\right)^{\frac{2}{3}} e^{-33.8(10^6/T)^{\frac{1}{3}}} \qquad (C_{pp} = 2.5 \times 10^6) \tag{2.28}
$$

Using the core condition for $Star^*$, $\rho_{core} = 45.7 g/cm^3$, $X = 0.7$, $T_{core} = 2.45 \times 10^7 K$, we can calculate the energy release rate of PP chain reaction $\varepsilon_{pp^*} = 58.6\, ergs/g/s$

If we assume that 100% of the Surface Luminosity is generated by the PPI chain. The number of PPI chain reaction per second would be:

$$
n = L_{tot}/E_{ppI} \tag{2.29}
$$

, where $E_{ppI} = 26.7 MeV$ is the energy released per reaction. We obtain that $n = 7.47 \times 10^{39}(s^{-1})$. Each reaction consumes four hydrogen atoms. Hence, the total number of hydrogen consumed

Table 2.2: The surface Condition of Thuban A comparing with $Srat^*$ [7]

Parameters	$star^*$	Thuban A
M_* (g)	$2.75M_\odot$	$2.80M_\odot$
R_* (cm)	$1.51R_\odot$	$3.40R_\odot$
L_* (ergs/s)	$83.14L_\odot$	$479L_\odot$
T_{eff} (K)	14170.8	10100
M^m	-0.21	-1.20
Spectral Type	B6	A0

per second is $4 \times n = 2.99 \times 10^{40}(s^{-1})$, corresponding to the mass of $4.99 \times 10^{13}(kg/s)$. The total amount of hydrogen of the $Star^*$ is $XM_{tot} = 3.83 \times 10^{30}(kg)$. All of the hydrogen will be consumed after 2.43×10^9 years. This is much shorter than the results obtained by equation 2.11, which was 1.82×10^{10} years. Hence, its impossible that the luminosity is produced solely by PPI chain.

CNO cycles is a series of nuclear reaction fusing proton with C, N, and O to produce Helium. The critical temperature needed for CNO cycles is larger than PP Chains because C, N, and O nuclei are highly charged. For massive stars ($M > 1.5M\odot$), the temperature is high enough so that the CNO cycles dominate the energy generation. The CNO cycles are summarized in figure 2.9. The energy generation rate of CNO cycles $\varepsilon_{CNO}(ergs/g/s)$is given by:[12].

$$\varepsilon_{CNO} = C_{CNO}\rho X X_{CNO}\left(\frac{10^6}{T}\right)^{\frac{2}{3}} e^{-152.3(10^6/T)^{\frac{1}{3}}} \quad (C_{CNO} = 9.5 \times 10^{28} \;\; X_{CNO} = 1/3Z) \tag{2.30}$$

Similarly, using the core conditions, we obtain that $\varepsilon_{CNO} = 1.62 \times 10^4\, ergs/g/s$. The ratio of the energy generation rate of PP Chains and CNO cycles is $\frac{\varepsilon_{CNO}}{\varepsilon_{pp}} = 276$. The CNO cycles dominates for $Star^*$.

2.3 Compare with A Real Star: Thuban A

Thuban is a single-lined spectroscopic binary system located in the constellation of Draco. A relatively inconspicuous star in the night sky of the Northern Hemisphere, it is historically significant as having been the north pole star from the 4th to 2nd-millennium BC[7]. The surface conditions of Thuban A is shown in table 2.3. Thuban's color is blue-white according to the spectral type of A0III, but much more luminous than $Star^*$. This is inconsistent with the properties of a main-sequence star if we put it on the H-R diagram. Thuban A has now ceased hydrogen fusion in its core and started to expand, making it a white giant star [7], indicating that Thuban has already spent more than ten billion years on the main sequence and just started to evolve to its next phase. Given good viewing conditions, Thuban can be seen with naked eyes ($m = 3.47^m$). Due to its location in relation to the Big Dipper asterism of Ursa Major, Thuban can be easily spotted in the night sky. The two inner stars of the 'dipper', Phecda and Megrez, point to Thuban, 15 degrees of arc from Megrez.

3. Conclusion

In this paper, we have modeled a $2.75M\odot$ main-sequence star. Its parameters data are in good agreement with the theory. The only thing that is unclear is the spectral type. We have obtained two different types for $Star^*$ determined by temperature and mass. The given surface condition for $Star^*$ maybe not be strictly derived from a theory. The mass for the main-sequence star with a temperature around 14000K should be higher than $2.75\odot$. Also, the interior Opacity data cannot fit very well with the hypothesis function. The Opacity data graph has some glitches. Thus, more thorough investigation and more information on how the data were generated are needed to fully evaluate the performance of our model.

Bibliography

[1] *The Pillars of Creation*. NASA, ESA and the Hubble Heritage Team, Feb 2018.

[2] Ionization energies, Sep 2020.

[3] B Type Main Sequence Star, Sep 2021.

[4] Magnitude (astronomy), Oct 2021.

[5] *Proxima Centauri*. Wikimedia Foundation, Nov 2021.

[6] *Star*. Wikimedia Foundation, Nov 2021.

[7] Thuban, Nov 2021.

[8] *Stars*. NASA, Nov 2021.

[9] Robert M. Geller, Roger A. Freedman, and William J. Kaufmann. *Universe*. Macmillan International Higher Education, 2019.

[10] Francis LeBlanc. *An introduction to stellar astrophysics*. Wiley, 2010.

[11] Manny. *What color is the hottest star What color is the coolest star*. Quora, 2020.

[12] James R. Sowell. *PHY3021 PowerPoint Lecture Slides*. Astronomy at Georgia Tech, Nov 2021.

Cover Image: [1]